Sensors and Actuators B 190 (2014) 715–722

Contents lists available at ScienceDirect

Sensors and Actuators B: Chemical

journal homepage: www.elsevier.com/locate/snb

Synthesis, inductive heating, and magnetoimpedance-based detection of multifunctional Fe_3O_4 nanoconjugates

J. Devkota[a], T.T.T. Mai[b,*], K. Stojak[a], P.T. Ha[b], H.N. Pham[b], X.P. Nguyen[b], P. Mukherjee[a], H. Srikanth[a], M.H. Phan[a,**]

[a] Department of Physics, University of South Florida, Tampa, FL 33620, USA
[b] Institute of Materials Science, Vietnam Academy of Science and Technology, 18 Hoang Quoc Viet, Cau Giay, Hanoi, Viet Nam

ARTICLE INFO

Article history:
Received 26 July 2013
Received in revised form 3 September 2013
Accepted 5 September 2013
Available online xxx

Keywords:
Functionalized magnetic nanoparticles
Drug delivery
Hyperthermia
Bio-detection

ABSTRACT

We report on the synthesis, inductive heating, and detection of a multifunctional nanosystem, which is composed of magnetite (Fe_3O_4) nanoparticles and two natural compounds, Alginate (Alg) and Curcumin (Cur). Alg was first absorbed onto the surface of Fe_3O_4 nanoparticles followed by loading of Cur in the nanoconjugate. The presence of Alg and Cur were confirmed by Fourier transform infrared spectroscopy, field-emission scanning electron microscopy, and transmission electron microscopy. The inductive heating capacity of the functionalized Fe_3O_4 nanoparticles was investigated under different alternating magnetic fields at 236 kHz, indicating that these nanoparticles are a promising agent for heat production in hyperthermia applications. Sensitive detection of the functionalized nanoparticles at various concentrations was carried out using a novel magnetoimpedance-based biosensor. High detection sensitivity was achieved at low particle concentration with saturated detection at an upper limit, as particle concentration exceeds a critical value. Our study indicates that the magnetic nanoconjugate of Fe_3O_4 nanoparticles encapsulated by Alg and Cur is a promising nanosystem for applications in drug delivery, hyperthermia, and biodetection.

1. Introduction

Magnetic nanoparticles (MNPs) have attracted special attention in various biomedical applications, such as molecular detection, drug delivery, hyperthermia, magnetic resonance imaging (MRI), and bioengineering [1–3]. The major requirements for MNPs to be suitable for biomedicine are non-toxicity biocompatibility, monodispersity, stability in colloidal media, high magnetic moment, and freedom from remanent field [3]. Surface modification and conjugation with a functional biopolymer can be used to tailor MNPs of special interest for a particular medical application. Research has demonstrated the potential benefits of therapies that integrate several distinct medical applications of MNPs. For example, hyperthermia could be made more effective if it were accompanied by targeted drug delivery after diagnosis [1,3]. Additionally, hyperthermia was shown to enhance the effectiveness of several kinds of anti-cancer drugs [4]. These observations suggest that designing a multifunctional MNP system would significantly advance the future of clinical medicine.

Among MNPs, superparamagnetic iron-oxide nanoparticles (Fe_3O_4 or γ-Fe_2O_3) have emerged as the most promising biomedical candidates as they are biocompatible, non-toxic, simple to fabricate, and remanence-free particles with high magnetic moment [5]. They can be made chemically stable by coating with a protective layer. Fe_3O_4 nanoparticles functionalized with suitable organic species were shown to be useful in MRI [6], drug delivery [2], hyperthermia [7], bioassay [8], magnetic purification [9], and other pharmaceutical applications [1,3]. Interestingly, Tran et al. [10] have recently shown that chitosan-based Fe_3O_4-Cur conjugate can be developed as a multifunctional nanosystem for applications in antibacterial and antiproliferative activities, drug delivery, and biodetection. This study raises a new possibility of developing a single system for multi-purpose applications of the functionalized MNPs. The effectiveness of MNPs could be enhanced when functionalized by a stable and well-established drug for a particular treatment in combination with quantitative detection by a high-sensitivity biosensing technique. It has been reported that a combination of magnetic sensors with functionalized MNPs offers a promising approach for a highly sensitive, simple, and quick detection of cancer cells and biomolecules [11–13]. This biodetection technique shows several advantages over conventional optical, electrochemical, and other methods. In light of these findings, it is essential to investigate the capacity of a magnetic biosensor in quantitative analysis of a potential nanoconjugate of varying

* Corresponding author.
** Corresponding author. Tel.: +1 813 974 4322.
E-mail addresses: trangmt@ims.vast.ac.vn (T.T.T. Mai), phanm@usf.edu (M.H. Phan).

0925-4005/$ – see front matter © 2013 Elsevier B.V. All rights reserved.
http://dx.doi.org/10.1016/j.snb.2013.09.033

concentration in a biologically-friendly environment for applications in targeted drug delivery, hyperthermia, and MRI.

In this work, we report on the engineering of functional magnetic nanoconjugates composed of superparamagnetic Fe_3O_4 nanoparticles coated by Alginate (Alg: a polysaccharide extracted from brown algae) and Curcumin (Cur: a yellow compound isolated from rhizome of *Curcuma longa L.* plant) for anti-cancer drug delivery and hyperthermia. In addition, we demonstrate the possibility of detecting these functionalized nanoparticles at low concentrations using a novel class of magnetic biosensor based on the giant magnetoimpedance (GMI) effect. In the nanoconjugate, Fe_3O_4 nanoparticles were used as heat media, Cur as a prototypical chemotherapy drug to achieve a combination effect in a system, and Alg to stabilize the system. The Cur is an anti-oxidant, anti-inflammatory, and one of the most promising anti-cancer drugs based on natural products, while the Alg is a natural polysaccharide with numerous biomedical applications [14,15]. The Fe_3O_4 MNPs were also used as magnetic biomarkers to detect Cur quantitatively by using the GMI biosensor whose working principle is based on the impedance change of its sensing element due to the fringe field of a magnetic biomarker. The GMI biosensor was chosen because it has been shown to be superior to other magnetic sensors [16–20]. It possesses high detection sensitivity and operates at ambient temperature [19], unlike a superconducting quantum interference device (SQUID)-based sensor which is highly sensitive, but requires cryogenic liquids to operate [21]. GMI sensors are also cost-effective, power-efficient, reliable, quick-response, and portable [22]. Our studies show that the Alg–Cur conjugated Fe_3O_4 nanoparticles are a very promising multifunctional nanosystem for applications in anti-cancer drug delivery, hyperthermia, and biomolecular detection. Since the MNPs explored in this study (Fe_3O_4) are widely used as MRI contrast agents, the GMI-based biosensing technique can also be used as a new, low-cost, fast and easy pre-detection method before MRI.

2. Experimental details

2.1. Synthesis and characterization of magnetic nanoconjugates

Magnetite nanoparticles were synthesized by co-precipitation of ferric and ferrous hydroxide in alkaline conditions as described in Mai et al. [23]. All of the raw materials used in the synthesis process were purchased commercially from Merck and used without further purification. Distilled water was used throughout all experiments, hereafter denoted as water only. The reaction equation is given as

$$2Fe^{3+} + Fe^{2+} + 8OH^- \rightarrow Fe_3O_4 + 4H_2O. \quad (1)$$

In a typical reaction, 4 mmol (0.65 g) of $FeCl_3$ and 2 mmol (0.3977 g) of $FeCl_2{\cdot}4H_2O$ were dissolved in 50 ml of HCl 2 M and added to a 250 ml three-necked flask containing a Teflon-coated magnetic stir bar. The mixture was vigorously stirred under N_2 purge. The temperature was kept at 70 °C throughout the process. As 80 ml of 2 M NH_4OH was dropped into the reaction mixture, a precipitate formed causing the entire solution to become black and reach a pH of 9. After 30 min of stirring, the product was washed several times with water until a pH of 7 was reached. The final product was washed with ethanol and dried at 60 °C for 24 h for characterization, or dispersed in water for further surface functionalization of Fe_3O_4, hereafter referred as Mag.

To coat with Alg, the Mag nanoparticles were dispersed in water with a concentration of 3 mg/ml. Separately, 0.1 g of Alg was added to 10 ml of water and stirred for 2 h until completely dissolved. Afterward, 30 ml of the Mag suspension was dropped slowly into the Alg solution under ultrasonic conditions at room temperature. The mixture of Mag and Alg was then magnetically stirred for 48 h. Finally, uncoated particles were separated by centrifugation and a magnetic fluid of 5 mg/ml Mag nanoparticles coated with Alg was obtained (Mag–Alg).

Cur was incorporated in the magnetic system of Mag–Alg nanoparticles as described by Ha et al. [24]. Firstly, 20 ml of 0.1 g/ml Mag–Alg magnetic fluid was added to a 200 ml flask containing a magnetic stir bar. In a separate container, 0.1 g of Cur was dissolved in 15 ml of ethanol and poured into the Mag–Alg magnetic fluid. The mixture was stirred in a closed vessel for 48 h followed by the removal of ethanol. The obtained product was centrifuged at 5000 rpm for 5 min to remove unencapsulated Cur. The final product (Mag–Alg–Cur) was stored at room temperature.

To characterize the synthesized samples (Mag and Mag–Alg–Cur MNPs), they were first dried at 60 °C under inert conditions. Their structural and morphological characterization was done using powder X-ray diffraction (XRD), field-emission scanning electron microscopy (FE-SEM), and transmission electron microscopy (TEM). Dynamic light scattering (DLS) was also used to determine the particle size distribution. The coating layer of Alg and presence of Cur were confirmed using Fourier transform infrared (FTIR) spectra. The magnetic properties of the Mag and Mag–Alg–Cur nanoparticles were characterized using a vibrating sample magnetometer (VSM).

2.2. Hyperthermia and biodetection experiments

In order to perform the hyperthermia experiment, the ferrofluid of Mag–Alg–Cur MNPs was diluted into three different concentrations. The magneto-inductive heating experiment was performed in the presence of an ac magnetic field of 50–70 Oe and with a frequency of 236 kHz produced by a commercial generator (RDO HFI 5 kW). The temperature of the ferrofluid was recorded using a commercial GaAs optical sensor (Opsens) with an accuracy of 0.3 °C. Details of the inductive heating of MNPs can be found elsewhere [23].

The sensing element of the biodetector was based on a commercial amorphous ribbon of composition $Co_{65}Fe_4Ni_2Si_{15}B_{14}$ (Metglas® 2714A) with dimensions 16 mm × 2 mm × 0.015 mm. This ribbon was prepared by a rapid quenching technique, and possesses high permeability, a vanishing coercivity, and near-zero magnetostriction. The ribbon was treated with an ~8% solution of HNO_3 for 24 h in order to improve detection sensitivity [25]. The Mag–Alg–Cur sample, originally prepared in a concentration of 5 mg/ml, was diluted in water and a certain volume of each concentration was drop-casted over the measurement area of the sensing element. The impedance of the plain sensing element (PSE) and that of the sensing element in the presence of various concentrations of Mag–Alg–Cur was measured over a length of 10 mm by a four-point measurement technique using an HP4192A impedance analyzer with a constant current of 5 mA and in the presence of axial dc magnetic field ranging up to ±120 Oe. The GMI ratio is defined as

$$\frac{\Delta Z}{Z} = \frac{Z(H) - Z(H_{max})}{Z(H_{max})} \times 100\% \quad (2)$$

The sensor's sensitivity was defined as the change in the maximum GMI ratio due to the presence of the MNPs with reference to the corresponding response of the plain probe as,

$$\Delta\eta = [MI]_{max,(PSE+MNPs)} - [MI]_{max,PSE}, \quad (3)$$

where $[MI]_{max} = [\Delta Z/Z]_{max}$ is the maximum value of the GMI ratio given in Eq. (2) at a given frequency.

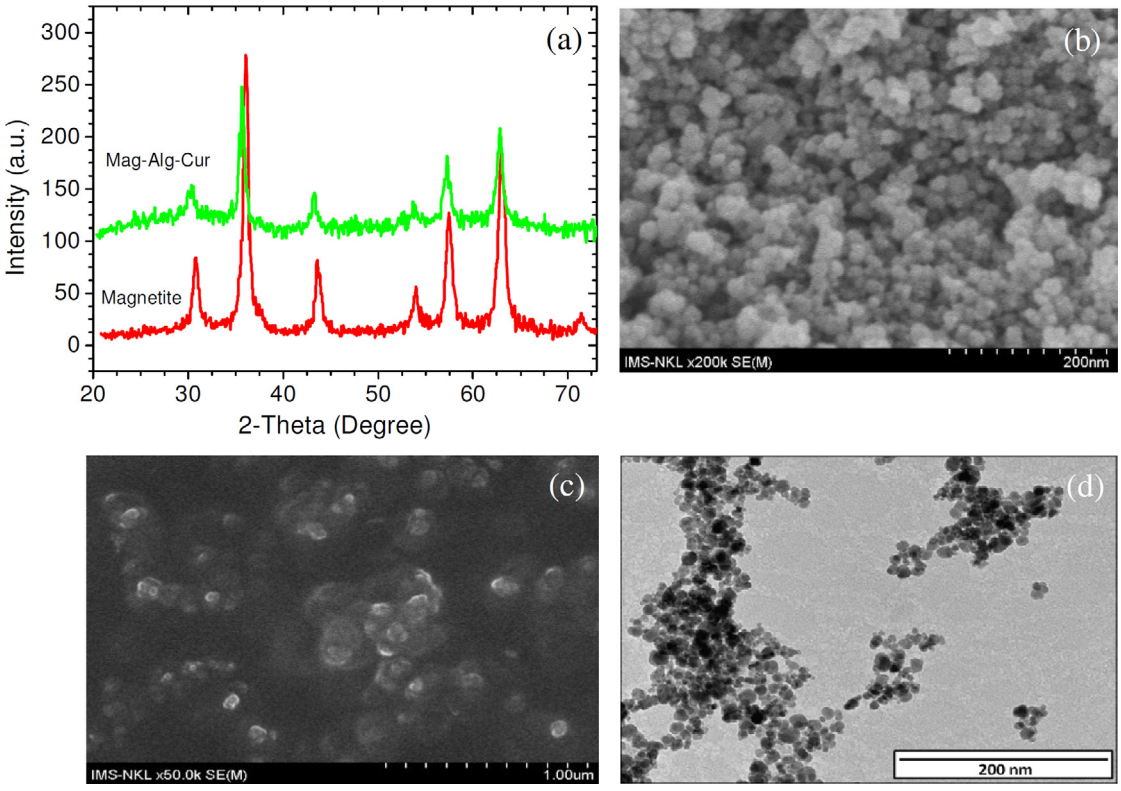

Fig. 1. (a) XRD spectra of Fe_3O_4 and Mag–Alg–Cur nanoparticles, SEM images of Fe_3O_4 nanoparticles (b) and Mag–Alg–Cur nanoparticles (c), and a TEM image of Mag–Alg–Cur nanoparticles (d).

3. Results and discussion

The structural and morphological characterizations of the synthesized Mag and Mag–Alg–Cur MNPs are shown in Fig. 1. The crystalline structures of Mag and Mag–Alg–Cur MNPs were analyzed using XRD at a wavelength of 1.54056 Å on a Siemens D5000. As shown in Fig. 1(a) for Mag MNPs, multiple peaks were observed at $2\theta = 31$, 36, 43, 53, 57, 63, and 74°, which are indexed as those of $Fe^{2+}Fe_2{}^{3+}O_4$ (JCPDS card No. 82-1533). These peaks were also observed in magnetic fluid samples containing the functionalized Mag–Alg–Cur MNPs, indicating that there was no chemical modification due to the encapsulation of Alg and loading of Cur. Fig. 1(b) shows a FE-SEM image of unmodified Mag MNPs, which are spherical, with a diameter of 10–15 nm. From a histogram analysis of the TEM image, the average size of these particles was estimated to be 10 ± 2.5 nm. The FE-SEM and TEM images shown in Fig. 1 (c–d) indicate that the addition of Alg and Cur increased the size of the Mag nanoparticles significantly, giving a final diameter of ~100 nm. The DLS spectrum showed a wide distribution of the Mag–Alg–Cur MNPs, with an average diameter of 120 ± 15 nm. This deviation in particle size could be due to clustering of the MNPs.

In order to confirm the coating of Alg and loading of Cur on Mag nanoparticles, the FTIR spectra of Mag, Alg, Cur, and Mag–Alg–Cur were performed using a Shimazdu FTIR with a wavenumber range of 400–4000 cm^{-1}; the results are shown in Fig. 2. The peak observed at 586 cm^{-1} is the characteristic peak of Fe–O–Fe in bulk Fe_3O_4 [26]. This peak was shifted to 574 cm^{-1} in the observed IR spectrum of the Mag–Alg–Cur nanoparticles. It could be explained by the coordination of iron in Fe_3O_4 and oxygen of $-COO^-$ groups in Alg [27]. For Alg, the broad bands between 2500 and 3300 cm^{-1} were attributed to the stretching vibration of hydrogen bond (O—H. . .H) [28]. The band at 1622 cm^{-1} was attributed to the stretching vibration of carboxylate groups ($-COO^-$). This band was also observed at 1626 cm^{-1} in the spectrum of Mag–Alg–Cur MNPs. As for Cur, a broad band at 3446 cm^{-1} was assigned to the stretching vibration of phenolic O—H group [29], which was observed to be overlapped with the stretching band of the hydrogen bond in Alg. In addition, typical peaks for stretching vibration of C=C of benzene ring and bending vibration of C—H bound to the benzene ring were observed at 1514 and 1430 cm^{-1}, respectively [29,30]. In the Mag–Alg–Cur spectrum, these peaks were shifted to 1503 and 1392 cm^{-1}, respectively. The peak at 861 cm^{-1}, the vibrational band of C—O in $-C-OCH_3$ of phenyl ring [29], was observed at 843 cm^{-1} in the Mag–Alg–Cur sample. The band at 1721 cm^{-1}, attributed to the vibration of the carbonyl bond (C=O) in Cur compound, was observed at 1757 cm^{-1} in the Mag–Alg–Cur spectrum. These

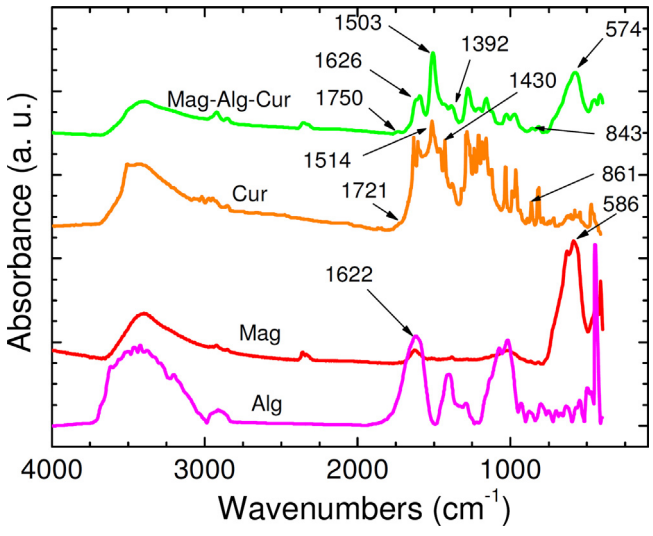

Fig. 2. FTIR spectra for Mag, Alg, Cur, and Mag–Alg–Cur.

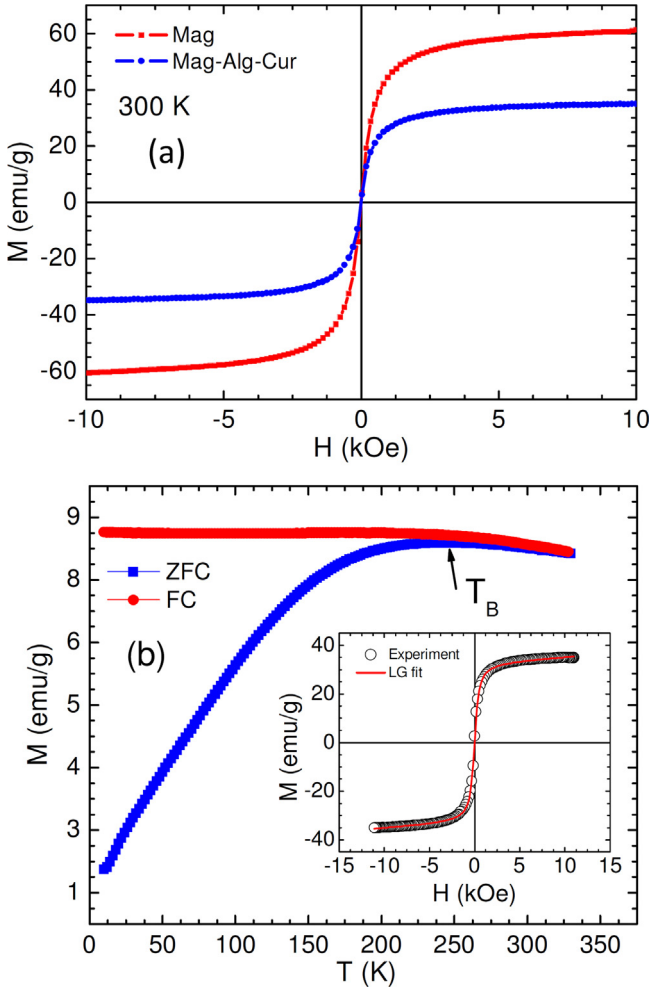

Fig. 3. (a) Room-temperature M–H curves of Mag and Mag–Alg–Cur nanoparticles; (b) temperature dependence of ZFC and FC magnetization for Mag–Alg–Cur nanoparticles. Inset shows the M–H curve at 300 K and its fit to the Langevin function for Mag–Alg–Cur nanoparticles.

variations could arise from some interaction between Cur and Alg and Mag and be involved in complexity of iron metal in Fe_3O_4 and C=O group in Cur [31]. The typical vibrational bands for these chemicals are summarized in Table 1. These results confirmed that Cur was loaded onto the Mag MNPs. The observation of all of the characteristic peaks of Mag, Alg, and Cur in the FTIR spectra of Mag–Alg–Cur MNPs confirmed the formation of a multifunctional magnetic system.

Fig. 3(a) shows the magnetic field dependence of magnetization (or magnetic hysteresis loops, M–H) taken at room temperature (300 K) for plain Mag and Mag–Alg–Cur MNPs. The saturation magnetization (M_S) of the plain Mag MNPs was determined to be about 60 emu/g, and reduced to about 37 emu/g (by ~35%) for the final Mag–Alg–Cur product. We note that the reduction of M_S due to encapsulation of Alg was only by 1–2% (not shown here). This implies that a significant mass of Cur was loaded onto Alg-encapsulated Mag MNPs, which was already confirmed by SEM and TEM images (Fig. 1). The large increase in the overall size of the particles due to the Cur coating could also minimize inter-particle interactions and consequently reduce the M_S of the final Mag-Alg–Cur product [32]. It is important to note that the M–H loops at 300 K did not show any coercivity (Fig. 3a), indicating a superparamagnetic nature of the functionalized MNPs. This result is consistent with the observation of the temperature dependence of the zero-field-cooled (ZFC) and field-cooled

Table 1
Summary of typical vibration bands.

	υ(—COO—) (cm^{-1})	υ(—C—O—) (cm^{-1})	υ(—O—H…H) (cm^{-1})	υ(O—H) (phenol) (cm^{-1})	υ(C=O) (cm^{-1})	υ(C=C) (cm^{-1})	υ(C—OCH$_3$) (cm^{-1})	υ(Fe—O—Fe) (cm^{-1})
Alg	1622	1031	2500–3300	–	–	–	–	–
Mag	–	–	2500–3300	–	–	–	–	586
Cur	–	–	–	3446	1721	1514; 1430	861	–
Mag–Alg–Cur	1626	1023	2500–3300	2500–3300	1750	1503; 1392	843	574

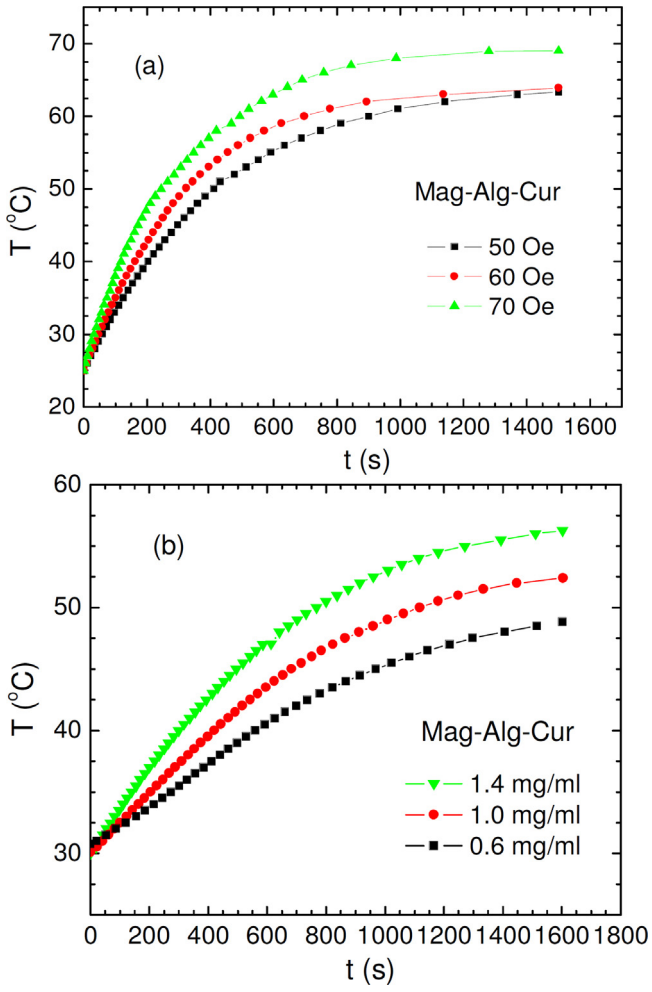

Fig. 4. Magneto-inductive heating experiments using Mag–Alg–Cur nanoparticles at different ac magnetic fields (a) and concentrations (b).

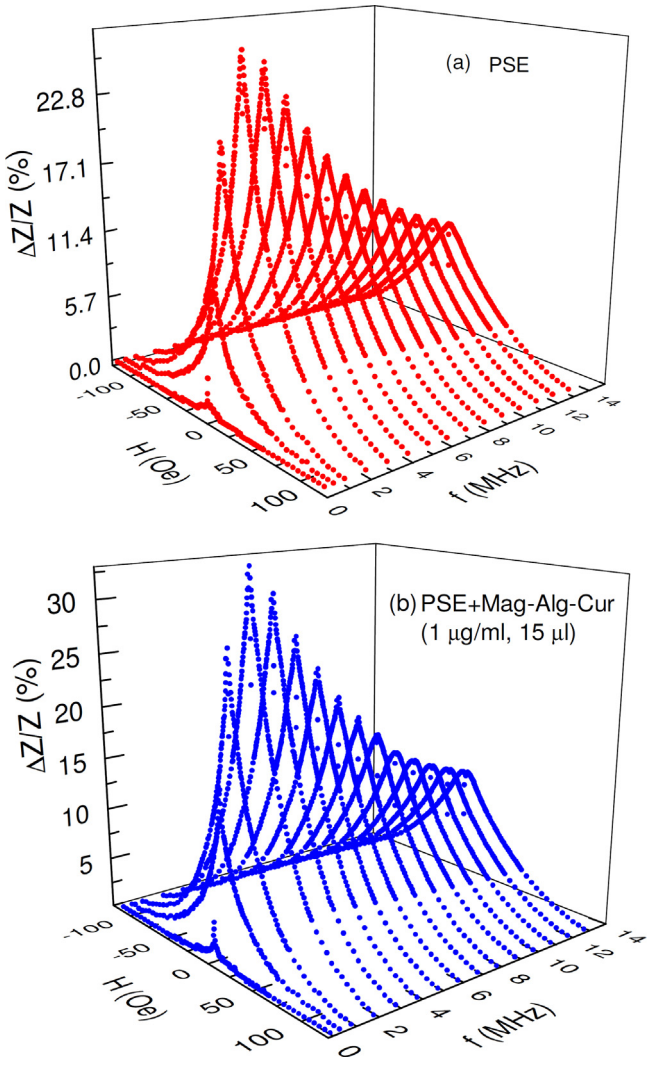

Fig. 5. Frequency and field dependences of GMI ratio (3D) for the plain ribbon and the ribbon with 15 μl of 1 μg/ml Mag–Alg–Cur nanoparticles.

(FC) magnetization (the M–T curves) in Fig. 3(b). The M–T curves show that while increasing temperature, this sample undergoes a transition from the ferromagnetic (blocked) to superparamagnetic state at $T_B \sim 245$ K (the so-called blocking temperature, which is often referred as to the peak of the ZFC M–T curve). The room-temperature superparamagnetic property of the functionalized MNPs has been further confirmed by the best fit of the M−H data at 300 K to the Langevin function [33] (see inset of Fig. 3b). The superparamagnetic properties of these MNPs are desirable for a wide range of biomedical applications. Further, we demonstrate below that these MNPs are promising for hyperthermia treatment and biodetection.

Fig. 4 shows the time dependence of the inductive heating experiment using Mag–Alg–Cur MNPs as the heating agent for different alternating magnetic fields (AMFs) (Fig. 4(a)) and different concentrations (Fig. 4(b)). For all the AMFs and concentrations, the temperature of Mag–Alg–Cur rose sharply, with time, up to ~800 s and then increased more slowly. As observed in Fig. 4(a), for a given concentration of 2 mg/ml, the change in temperature increased with the amplitude of the AMF, from a maximum of ~55 °C at 50 Oe up to a maximum of ~68 °C at 70 Oe. As the particle concentrations were increased and measurements were repeated while holding the AMF at a constant value of 65 Oe, a similar effect was observed as shown in Fig. 4(b). To be specific, the maximum values of ~45, 50, and 55 °C were observed respectively for 0.6, 1.0, and 1.4 mg/ml of the Mag–Alg–Cur nanoconjugate. These observations show that the Mag–Alg–Cur nanoconjugate is a promising agent for applications in hyperthermia. We note here that while similar heating curves were observed for both types of Mag- and Mag–Alg–Cur containing ferrofluids, the initial temperature increase and saturated heating temperature of Mag were higher than those of Mag–Alg–Cur, due to the higher concentration of magnetic particles in the former sample than in the latter one.

Finally, to testify to the possibility of using these functionalized MNPs for molecular detection at room temperature, when combined with the novel GMI biosensor, we measured the frequency and magnetic field dependences of GMI ratio ($\Delta Z/Z$) for the plain sensing element (PSE) and the PSE with 15 μl of 1 μg/ml Mag–Alg–Cur MNPs. The results obtained are shown in Fig. 5. As expected, the GMI profiles for the PSE (Fig. 5(a)) and PSE + Mag–Alg–Cur (Fig. 5(b)) were observed to possess similar features. For both samples, the GMI ratio increased sharply with frequency, reached a peak value at ~2 MHz, and then decreased slowly for higher frequencies. The frequency dependence of the GMI profile can be explained by considering the dependence of the impedance on transverse permeability via the skin effect, as detailed in previous works [16,19].

From a biosensing perspective, it is worth noting that the $[\Delta Z/Z]_{max}$ of PSE + Mag–Alg–Cur (Fig. 5(a)) was higher than that of PSE alone (Fig. 5(b)). We recall that an amorphous ribbon used as a sensing element in GMI biosensors may be subject to biochemical

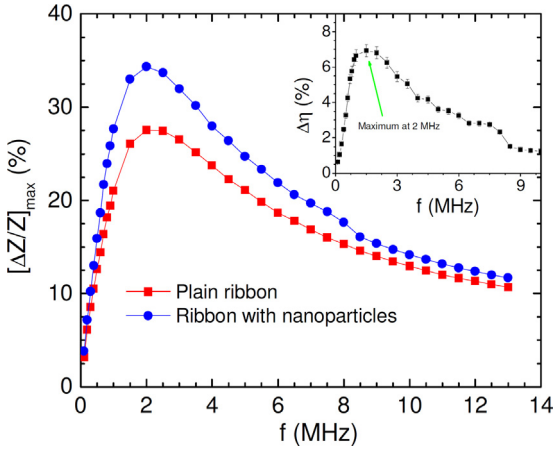

Fig. 6. Frequency dependence of $[\Delta Z/Z]_{max}$ for the plain ribbon and the ribbon with Mag–Alg–Cur nanoparticles. Inset shows the difference between their peak values at various frequencies.

corrosion when a solution is drop-casted on the surface of the ribbon [34]. Therefore, it is necessary to examine the GMI signal of PSE before and after drop-casting a solution containing MNPs, as well as after completely removing the MNP-containing solution from the ribbon surface. In the present study, since the functionalized MNPs were dispersed in water, we carefully checked GMI signal of PSE without water, with water, with water containing MNPs, and after removing the MNP-containing water solution. The GMI signals were recorded to be almost identical for the cases of PSE without water, with water, and after removing the MNP-containing water, indicating a negligible corrosion effect of water on the presently used ribbon. This is in good agreement with a previous study by Kurlyandskaya et al. [34] that showed the negligible corrosion effect of water on a Co-based ribbon. For clarification, in this paper we only report on the comparison of the GMI signals of the two cases: plain ribbon without water (e.g. PSE) and the PSE with water containing the functionalized MNPs (e.g. PSE + Mag–Alg–Cur).

For a quantitative determination of the increase in $[\Delta Z/Z]_{max}$ due to the presence of the Mag–Alg–Cur, the frequency dependence of the $[\Delta Z/Z]_{max}$ for PSE and PSE + Mag–Alg–Cur was studied, the results of which are shown in Fig. 6. For both samples, the $[\Delta Z/Z]_{max}$ was observed to possess peaks at $f \sim 2$ MHz. Relative to PSE, the higher values of $[\Delta Z/Z]_{max}$ due to the presence of the MNPs were found over the whole frequency range. The inset of Fig. 6 shows the calculated difference in the $[\Delta Z/Z]_{max}$ for these two cases based on Eq. (2) over the whole frequency range. A maximum increase of $[\Delta Z/Z]_{max}$, with $\Delta\eta_{max} \sim 6.5\%$ was obtained at $f \sim 2$ MHz, where their peaks were observed. The above results suggest that these functionalized MNPs can be detected by a GMI biosensor over a wide range of frequencies, with the highest detection sensitivity achieved at $f \sim 2$ MHz. This demonstrates the detection flexibility of the GMI biosensor in detecting different biomarkers to be used in hyperthermia experiments at various frequencies. This change in the GMI ratio due to the presence of the functionalized Mag–Alg–Cur MNPs can be explained by the effect of their fringe fields on the superposition of the applied axial dc magnetic field and the induced transverse ac field (due to an ac current flowing along the axis of the ribbon) [16]. Especially at sufficiently high frequencies, the skin effect of the ribbon is very strong, rendering surface highly sensitive to its electrical and magnetic environment. Therefore, the presence of even a low concentration of MNPs alters the impedance of the ribbon to a great extent, which ultimately leads to a sensitive detection of biomolecules attached to a magnetic biomarker [16,19].

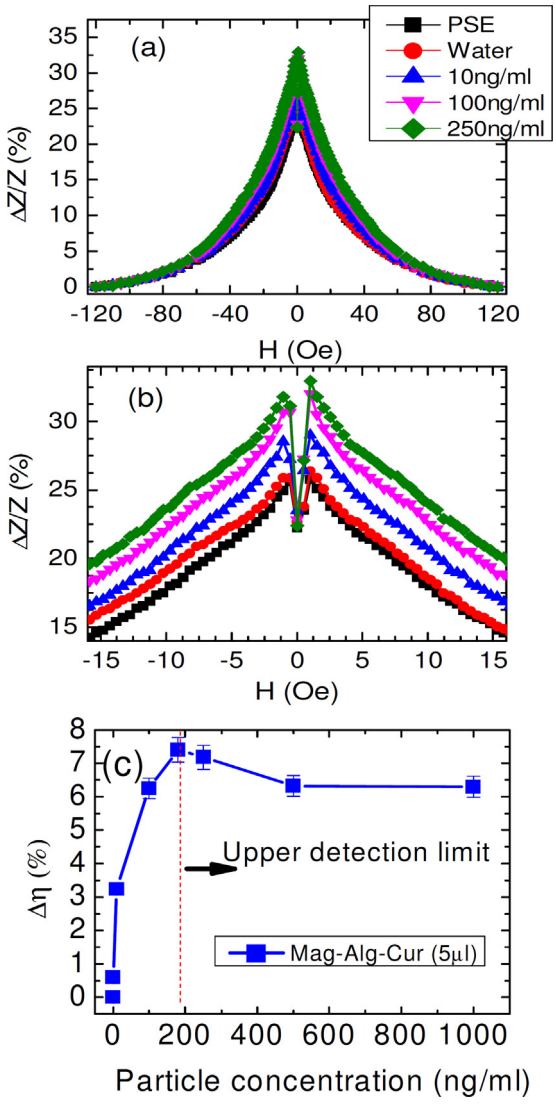

Fig. 7. Magnetic field dependence of GMI ratio for various concentrations of Mag–Alg–Cur nanoparticles (a); the low-field enlarged graph (b), and concentration dependence of detection sensitivity of the ribbon-based GMI sensor in detecting Mag–Alg–Cur nanoparticles (c).

Fig. 7(a) shows the field dependence of the GMI ratio for various concentrations of Mag–Alg–Cur at $f = 1.5$ MHz. Fig. 7(b) is its enlarged view in a narrow field range. We selected a frequency of 1.5 MHz for this experiment because the difference in the GMI responses of PSE with and without Mag–Alg–Cur was largest at this frequency. As observed in enlarged Fig. 7(b), the change in the GMI ratio for water as compared to the PSE was negligible while it increased significantly with concentrations of the Mag–Alg–Cur nanoconjugate. The concentration dependence of the GMI ratio in a wide range is better illustrated in Fig. 7(c), where $\Delta\eta$ of $[\Delta Z/Z]_{max}$ for different concentrations of Mag–Alg–Cur was obtained according to Eq. (3). This difference $\Delta\eta$ defines the sensitivity of the sensing element in detecting particular concentration of the Mag–Alg–Cur nanoconjugate. It is clear from Fig. 7(c) that the $\Delta\eta$ increased from zero for PSE, up to about 7% for 200 ng/ml of Mag–Alg–Cur, and remained almost constant beyond this concentration. We have recently reported a similar trend with non-functionalized Fe_3O_4 nanoparticles [19]. The increase in GMI ratio with concentration of biomarkers and existence of an upper critical concentration have also been reported by Chiriac et al. [35] and Martin et al. [36]. However, Wang et al. [20] have observed a

decrease in the GMI ratio of the sensing element due to the presence of MNPs. This difference likely arises from the difference in the superposition effect of the fringe field of MNPs, the induced transverse ac field, and the dc external field. In the former case, the presence of the fringe field of MNPs could compensate the decrease in the GMI ratio caused by stray fields due to the surface roughness of the sensing element, thus enhancing the effective magnetic permeability and the GMI ratio [19,25]. In the latter case, however, for sensing elements with a smooth surface like a thin film, the presence of the fringe field of MNPs could cause magnetic inhomogeneity, thus reducing the effective magnetic permeability and the GMI ratio [20]. In both cases, the change in GMI (its absolute value) with the presence of MNPs was exploited for the biodetection purpose.

It has been noted that the detection sensitivity of a magnetic biosensor is considerably reduced upon increasing distance between the sensing element and MNPs [12,13]. Functionalizing the surface of MNPs with biopolymer layers increases significantly the effective diameter of the particles and hence the distance between the sensing element and the MNPs. As a result, a significant decrease in the detection sensitivity of the biosensor is often observed when detecting functionalized MNPs, with reference to non-functionalized MNPs [13]. However, as compared to the detection described by us in Ref. [19] for the non-functionalized Fe_3O_4 nanoparticles ($\Delta\eta \sim 2\%$), we have achieved a higher detection capacity (~3 times) for the functionalized Fe_3O_4 nanoparticles (Fe_3O_4 nanoparticles coated with Alg and Cur) in the present study ($\Delta\eta \sim 7\%$). This is not very surprising given that unlike the case [19], the ribbon was treated with HNO_3 in the present case, in order to create nanoholes on the surface of the ribbon. As demonstrated in our previous study [25], the presence of these nanoholes enhanced magnetic interactions between the magnetic signal near the surface of the ribbon and the fringe field of MNPs located on the surface, which, in effect, increased the overall detection capacity of the biosensor to the MNPs. These results indicate that the biosensing technique that we have advanced is well suited for highly sensitive detection of functionalized MNPs for a wide range of applications in biomedicine.

4. Conclusions

Multifunctional nanoconjugates of magnetite nanoparticles coated with Alginate and Curcumin were successfully synthesized, characterized, and tested for drug delivery and hyperthermia heating. The nanoconjugates were detected by using a high sensitivity GMI biosensor at room temperature. The detection of nanoconjugates was found to be sensitive in a low concentration range and had an upper limit for high concentrations. Our study is of practical importance in designing a multifunctional magnetic nanoparticle system for multiple applications in biomedicine, with special emphasis on quantitative drug delivery and hyperthermia.

Acknowledgements

The research at USF was supported by the Florida Cluster for Advanced Smart Sensor Technologies (FCASST) and by USAMRMC through grant numbers W81XWH-07-1-0708 and W81XWH1020101/3349. The research at IMS-VAST was supported by the National Foundation for Science and Technology Development of Vietnam through grant numbers 103.02-2011.31 (NXP) and 106.99-2012.43 (HPT). The members of Biomedical Nanomaterials Lab and IMS-VAST Key Laboratory are acknowledged for facilities' support. Metglas/Hitachi Metals America is also acknowledged for providing Cobalt based METGLAS® 2714A ribbons.

References

[1] Q.A. Pankhurst, J. Connolly, S.K. Jones, J. Dobson, Applications of magnetic nanoparticles in biomedicine, Journal of Physics D: Applied Physics 36 (2003) R167–R181.
[2] B. Chertok, B.A. Moffat, A.E. David, F.Q. Yu, C. Bergemann, B.D. Ross, V.C. Yang, Iron oxide nanoparticles as a drug delivery vehicle for MRI monitored magnetic targeting of brain tumors, Biomaterials 29 (2008) 487–496.
[3] M. Colombo, S. Carregal-Romero, M.F. Casula, L. Gutierrez, M.P. Morales, I.B. Bohm, J.T. Haverhagen, D. Prosperi, W.J. Parak, Biological applications of magnetic nanoparticles, Chemical Society Reviews 41 (2012) 4306–4334.
[4] S. Brule, M. Levy, C. Wilhelm, D. Letourneur, F. Gazeau, C. Menager, C. Le Visage, Doxorubicin release triggered by alginate embedded magnetic nanoheaters: a combined therapy, Advanced Materials 23 (2011) 787.
[5] A. Figuerola, R. Di Corato, L. Manna, T. Pellegrino, From iron oxide nanoparticles towards advanced iron-based inorganic materials designed for biomedical applications, Pharmacological Research 62 (2010) 126–143.
[6] M.F. Bellin, MR contrast agents, the old and the new, European Journal of Radiology 60 (2006) 314–323.
[7] A. Jordan, P. Wust, H. Fahling, W. John, A. Hinz, R. Felix, Inductive heating of ferrimagnetic particles and magnetic fluids – physical evaluation of their potential for hyperthermia, International Journal of Hyperthermia 9 (1993) 51–68.
[8] T. Osaka, T. Matsunaga, T. Nakanishi, A. Arakaki, D. Niwa, H. Iida, Synthesis of magnetic nanoparticles and their application to bioassays, Analytical and Bioanalytical Chemistry 384 (2006) 593–600.
[9] M. Fuentes, C. Mateo, A. Rodriguez, M. Casqueiro, J.C. Tercero, H.H. Riese, R. Fernandez-Lafuente, J.M. Guisan, Detecting minimal traces of DNA using DNA covalently attached to superparamagnetic nanoparticles and direct PCR-ELISA, Biosensors and Bioelectronics 21 (2006) 1574–1580.
[10] D.L. Tran, G.D. Pham, X.P. Nguyen, D.H. Vu, N.T. Nguyen, V.H. Tran, T.T. Trang Mai, H.B. Nguyen, Q.D. Le, T.N. Nguyen, T.C. Ba, Some biomedical applications of chitosan-based hybrid nanomaterials, Advances in Natural Sciences: Nanoscience and Nanotechnology 2 (2011) 45004.
[11] D.R. Baselt, G.U. Lee, M. Natesan, S.W. Metzger, P.E. Sheehan, R.J. Colton, A biosensor based on magnetoresistance technology, Biosensors and Bioelectronics 13 (1998) 731.
[12] S.X. Wang, G.X. Li, Advances in giant magnetoresistance biosensors with magnetic nanoparticle tags: review and outlook, IEEE Transaction on Magnetics 44 (2008) 1687–1702.
[13] J. Llandro, J.J. Palfreyman, A. Ionescu, C.H.W. Barnes, Magnetic biosensor technologies for medical applications: a review, Medical and Biological Engineering and Computing 48 (2010) 977–998.
[14] B.B. Aggarwal, B. Sung, Pharmacological basis for the role of curcumin in chronic diseases: an age-old spice with modern targets, Trends in Pharmacological Sciences 30 (2009) 85–94.
[15] K.Y. Lee, D.J. Mooney, Alginate: properties and biomedical applications, Progress in Polymer Science 37 (2012) 106–126.
[16] G.V. Kurlyandskaya, M.L. Sanchez, B. Hernando, V.M. Prida, P. Gorria, M. Tejedor, Giant-magnetoimpedance-based sensitive element as a model for biosensors, Applied Physics Letters 82 (2003) 3053–3055.
[17] A. Kumar, S. Mohapatra, V. Fal-Miyar, A. Cerdeira, J.A. Garcia, H. Srikanth, J. Gass, G.V. Kurlyandskaya, Magnetoimpedance biosensor for Fe_3O_4 nanoparticle intracellular uptake evaluation, Applied Physics Letters 91 (2007) 143902.
[18] L. Chen, C.C. Bao, H. Yang, D. Li, C. Lei, T. Wang, H. Hu, M. He, Y. Zhou, D. Cui, A prototype of giant magnetoimpedance-based biosensing system for targeted detection of gastric cancer cells, Biosensors and Bioelectronics 26 (2011) 3246–3253.
[19] J. Devkota, C. Wang, A. Ruiz, S. Mohapatra, P. Mukherjee, H. Srikanth, M.H. Phan, Detection of low-concentration superparamagnetic nanoparticles using an integrated radio frequency magnetic biosensor, Journal of Applied Physics 113 (2013) 140701.
[20] T. Wang, Y. Zhou, C. Lei, J. Lei, Z. Yang, Development of an ingenious method for determination of Dynabeads protein A based on a giant magnetoimpedance sensor, Sensors and Actuators B: Chemical 186 (2013) 727–733.
[21] D. Drung, C. Assmann, J. Beyer, A. Kirste, M. Peters, F. Ruede, et al., Highly sensitive and easy-to-use SQUID sensors, IEEE Transactions on Applied Superconductivity 17 (2007) 699–704.
[22] G.V. Kurlyandskaya, Giant magnetoimpedance for biosensing: advantages and shortcomings, Journal of Magnetism and Magnetic Materials 321 (2009) 659–662.
[23] T.T.T. Mai, P.T. Ha, H.N. Pham, T.T.H. Le, H.L. Pham, T.B.H. Phan, D.L. Tran, X.P. Nguyen, Chitosan and O-carboxymethyl chitosan modified Fe3O4 for hyperthermic treatment, Advances in Natural Sciences: Nanoscience and Nanotechnology 3 (2012) 015006.
[24] P.T. Ha, T.M.N. Tran, H.D. Pham, Q.H. Nguyen, X.P. Nguyen, The synthesis of poly(lactide)-vitamin E TPGS (PLA-TPGS) copolymer and its utilization to formulate a curcumin nanocarrier, Advances in Natural Sciences: Nanoscience and Nanotechnology 1 (2010) 15012.
[25] J. Devkota, A. Ruiz, P. Mukherjee, H. Srikanth, M.H. Phan, Magneto-impedance biosensor with enhanced sensitivity for highly sensitive detection of Nanomag-D beads, IEEE Transactions on Magnetics 49 (2013) 4060.
[26] R.M. Cornell, U. Schwertmann, The Iron Oxide: Structure, Properties, Reactions, Occurrence and Uses, 1st ed., Wiley-VCH, Weinheim, Cambridge, 1996.

[27] A. Zhu, L. Yuan, T. Liao, Suspension of Fe_3O_4 nanoparticles stabilized by chitosan and o-carboxymethylchitosan, International Journal of Pharmaceutics 350 (2008) 361–368.
[28] X.Q. Xu, H. Shen, J.R. Xu, M.Q. Xie, X.J. Li, The colloidal stability and core–shell structure of magnetite nanoparticles coated with alginate, Applied Surface Science 253 (2006) 2158–2164.
[29] M.M. Yallapu, M. Jaggi, S.C. Chauhan, β-Cyclodextrin-curcumin self-assembly enhances curcumin delivery in prostate cancer cells, Colloids and Surfaces B: Biointerfaces 79 (2010) 113–125.
[30] P. Wang, W. Hu, W. Su, Molecularly imprinted poly (methacrylamide-co-methacrylic acid) composite membranes for recognition of curcumin, Analytica Chimica Acta 615 (2008) 54–62.
[31] B. Zebib, Z. Mouloungui, V. Noirot, Stabilization of Curcumin by complexation with divalent cations in glycerol/water system, Bioinorganic Chemistry and Applications 2010 (2010) 292760.
[32] S. Pal, M. Morales, P. Mukherjee, H. Srikanth, Synthesis and magnetic properties of gold coated iron oxide nanoparticles, Journal of Applied Physics 105 (2009) 07B504.
[33] B.D. Cullity, Introduction to Magnetic Materials, Addison-Wesley, Reading, MA, 1972, pp. 94, 389–414.
[34] G.V. Kurlyandskaya, V. Fal Miyar, A. Saad, E. Asua, J. Rodriguez, Giant magnetoimpedance: a label-free option for surface effect monitoring, Journal of Applied Physics 101 (2007) 54505–54509.
[35] H. Chiriac, M. Tibu, A.-E. Moga, D.D. Herea, Magnetic GMI sensor for detection of biomolecules, Journal of Magnetism and Magnetic Materials 293 (2005) 671–676.
[36] V.C. Martins, F.A. Cardoso, J. Loureiro, M. Mercier, J. Germano, S. Cardoso, R. Ferreira, L.P. Fonseca, L. Sousa, M.S. Piedade, P.P. Freitas, Integrated spintronic platforms for biomolecular recognition detection, AIP Conference Proceedings 1025 (2008) 150–175.

Biographies

Jagannath Devkota received his M.S. degree in Physics from the University of Southern Mississippi, Hattiesburg in 2010. He is currently pursuing his Ph.D. in Applied Physics at the University of South Florida. His current research is focused on developing a new generation of magnetic biosensors using the giant magnetoimpedance effect of soft ferromagnetic materials. His other research interests include novel nanodevices for biomedical and energy applications.

Thi Thu Trang Mai received her B.S. degree in Chemical Engineering from Hanoi University of Science and Technology and M.S. degree in Drug Development from the University of Science and Technology of Hanoi. She presently works at the Laboratory of Biomedical Nanomaterials, Institute of Materials Science, Vietnam Academy of Science and Technology (VAST). Her current research is focusing on the development of advanced nanomaterials system based on magnetic nanoparticles for biomedical applications.

Kristen Stojak received her M.S. degree in Materials Science and Engineering from the University of South Florida (USF) in 2013. She is currently a Ph.D. student of the Department of Physics at USF. Her research interests include the synthesis and characterization of magnetic nanoparticles, magnetic polymer nanocomposites and magnetic carbon nanotubes for applications ranging from RF and microwave sensors to bioengineering.

Phuong Thu Ha received her Ph.D. degree in Physical Chemistry from the Institute of Chemistry, Vietnam Academy of Science and Technology (VAST). After two years of Postdoctoral fellowship at the French Atomic Energy Commission (CEA) and the Tokyo Institute of Technology, she joined the Institute of Materials Science, VAST. Her current research interest is the development of drug delivery nanosystems including preparation, structural characterization, and biological activities.

Hong Nam Pham received his B.S. degree in Materials Science from Hanoi University of Science. He currently works at the Laboratory of Biomedical Nanomaterials, Institute of Materials Science, Vietnam Academy of Science and Technology (VAST). His current research is focused on the fabrication and characterization of magnetic nanoparticles for biomedical applications.

Xuan Phuc Nguyen received his Ph.D. degree from Jagiellonian University and Habilitatus Degree from the Institute of Nuclear Physics in Condensed Matter Physics, Cracow, Poland. He works at the Institute of Materials Science, Vietnam Academy of Science and Technology (VAST). He is currently interested in the physical properties and biomedical applications of magnetic-nanoparticle based systems.

British Mukherjee received his Ph.D. in Electrical Engineering from the State University of New York at Buffalo. Following a postdoctoral fellowship at the Los Alamos National Laboratory, he joined the University of South Florida in Tampa where he is currently Professor and Chair of the Department of Physics. His research interests include innovations in pulsed laser ablation and new laser-assisted plasma processes for the growth of thin films and nanostructures of technologically significant materials, and the exploration of novel optical techniques for high-resolution, in situ plasma imaging. Materials of interest include super-hard materials, magnetic materials, thermoelectric materials, multiferroics, superconductors, and compound semiconductors for solar cells.

Hariharan Srikanth received his Ph.D. in Physics from the Indian Institute of Science. After two years of postdoctoral research at Northeastern University and two years as a Research Assistant Professor at the University of New Orleans, he joined The University of South Florida where he is currently a Professor of Physics. His research interests are on nanostructured magnetic materials, electromagnetic and thermomagnetic phenomena, complex oxides and other correlated electron materials.

Manh-Huong Phan received his Ph.D. in Engineering Physics from the University of Bristol, United Kingdom. Presently he works in the Department of Physics at the University of South Florida. His research interests include the underlying physics and applications of magnetic nanomaterials, with a focus on the exploration of advanced nanomaterials with giant magnetocaloric and magnetoimpedance effects for energy-efficient magnetic refrigeration and smart sensor technologies.